Damage Resistance of a Co-cured Composite Wing Box to Low-Velocity Impact

1 Introduction

- Composite laminates have poor resistance to low-velocity impact
  - Caused by dropping tools
- Delamination is a serious damage
  - Hard to detect through visual inspection → Causes earlier buckling failure
- Impact on a small specimen
  - Regarded as quasi-static procedure → Contact force and plate response are in phase
  - The spring-mass model for simulating
- Low-velocity impacts were applied to an aircraft wing box fabricated by co-curing its spar and skin

Delamination threshold load (DTL)
Energy absorbed
Permanent indentation

} Primary parameters for the damage resistance of composite laminates to low-velocity impact

2 Composite Wing Boxes & Experiment Setup

- Two wing boxes fabricated using carbon fibre-reinforced plastic composites:
  - First wing box is for the responses of the panel to low-velocity impacts
  - Second one is tested with the static bending load (five typical points) → Effect of the impact damage on structural strength

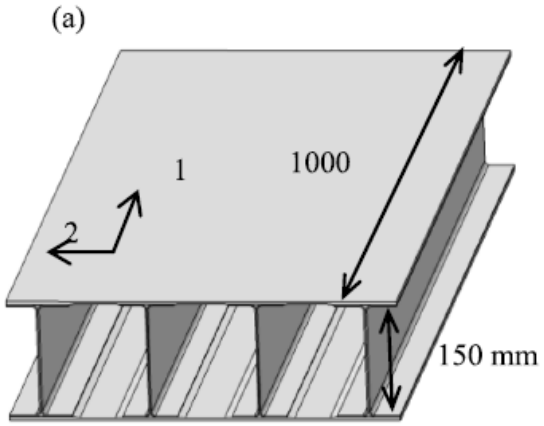

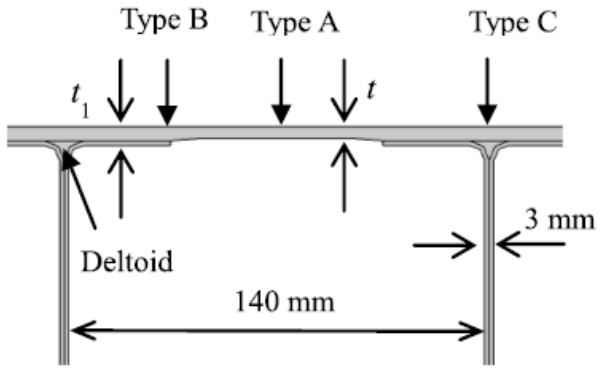

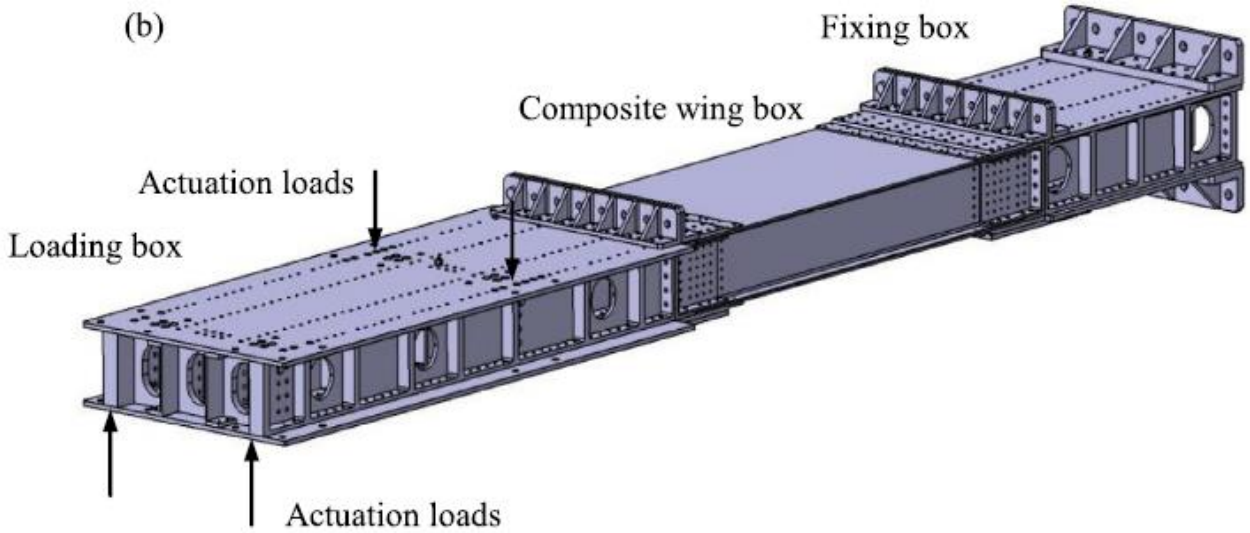

Wing Box: comprises skins and spars.

- Each spar consists of two beams with a channel cross-section.
- The deltoid region is formed by the two beams
- The skin was filled with the fibre bundle.
- Stacking sequence is $[45/-45/0_2/(45/-45)_2 90]s$
- The thickness of the skin is 3.76mm
- The skin and the spar were co-cured.

- Three types of sites were subjected to the low-velocity impact:
  - **Type A:** at the bay between the spars
    - To demonstrate the improved DTL model
  - **Type B:** at the edge of the flange
  - **Type C:** exactly over the web.

} Region 2 & Region 3

- The wing box was connected to two steel boxes
  - Fixed at its two ends
- Four hydraulic actuators → To exert torsional and bending loading
- A drop tower → To produce the low-velocity impact
- The contact force was measured with the dynamic force sensor.
- The mass of the impactor can be adjusted by adding weights (5.3-10.4kg).

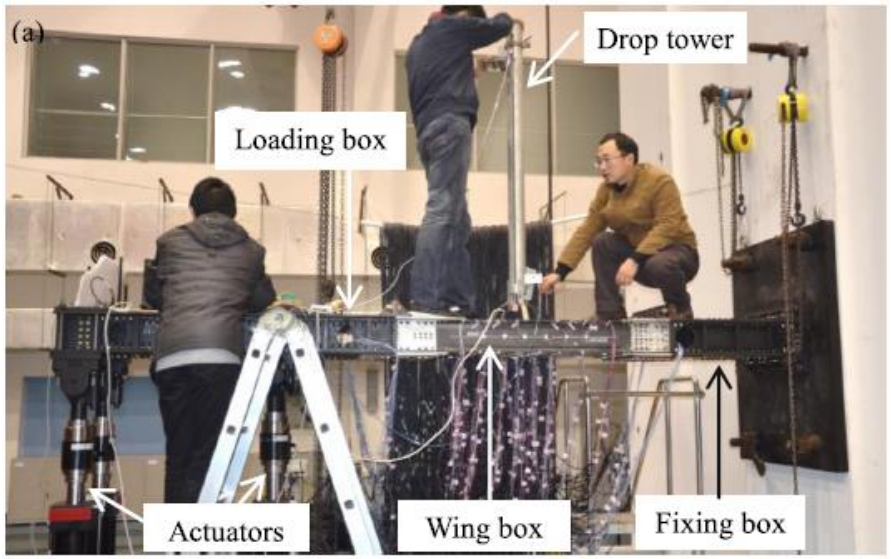

3 Results of Impact Tests

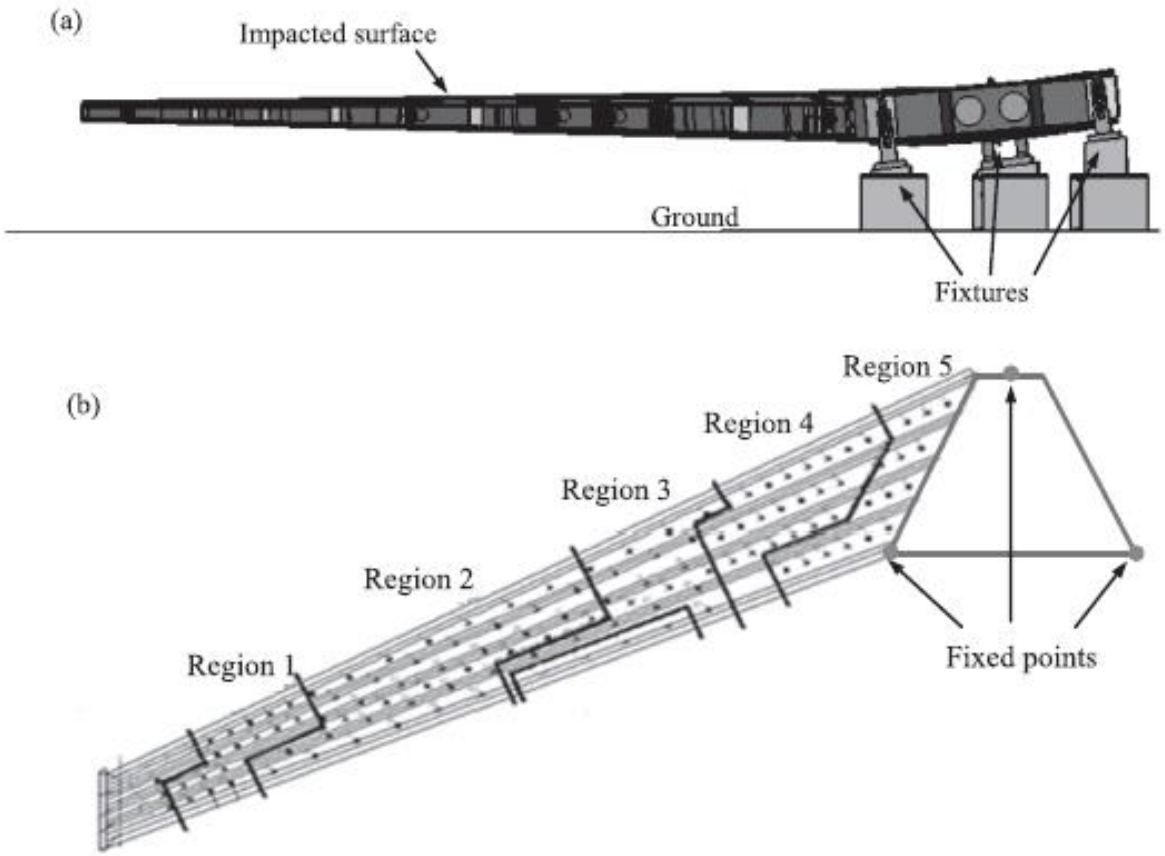

Table 1
Layup parameters of the regions of the composite horizontal tail.

Regions	Plies amount	t/mm	t_1/mm
Region 2	20	3.76	6.03
Region 3	24	4.51	7.22
Region 5	40	7.52	3.61

Composite horizontal tail: **(a)** fixtures setup **(b)** regions subjected to impact

3.1 Impact of Type A

- Energy ranging from 10 J to 60 J
- Peak force is lower than DTL of the 15J impact (~5290 N)
- Less than 5290 N → Significant damage does not ocur

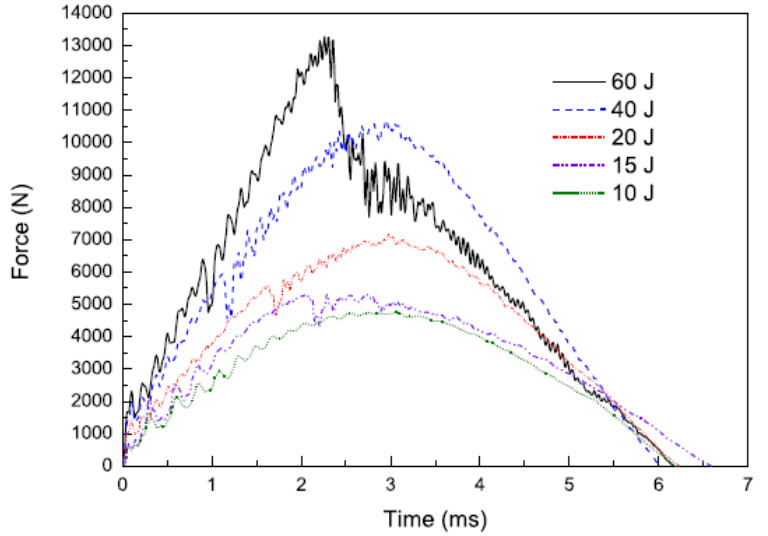

Fig. 4. Contact force histories of the type-A impact on the wing box.

- Sharp drop in each curve for the impact greater than 10 J
- The dramatic load drop at the peak in the 60-J curve :
  - Major portion of the delamination damage.
  - Crushing of the matrix and breakage of fibre at point
  - Significant indentation was then observed

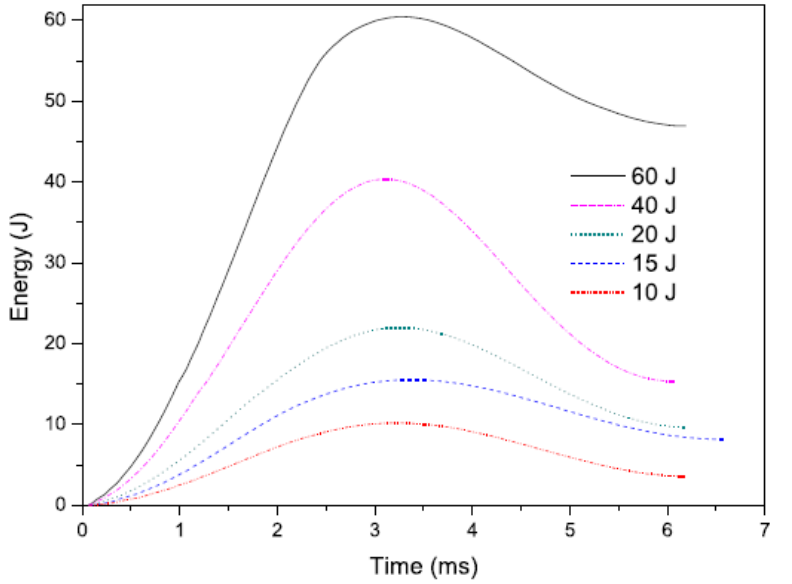

Fig. 7. Time histories of energy absorbed in the type-A impact on the wing box.

3.2. Impact of Type B

- Ranging from 10 J to 65 J
- Average DTL is equal to 6872 N
- A sharp drop appears when impact energy >10 J

3.3 Impact of Type C

- Ranging from 10 J to 60 J
- Secondary bump after the peak in the 40J & 60J
- No sharp drop occurs in the contact force
- The horizontal tail has lower stiffness than wing box → Impact energy was absorbed over structure

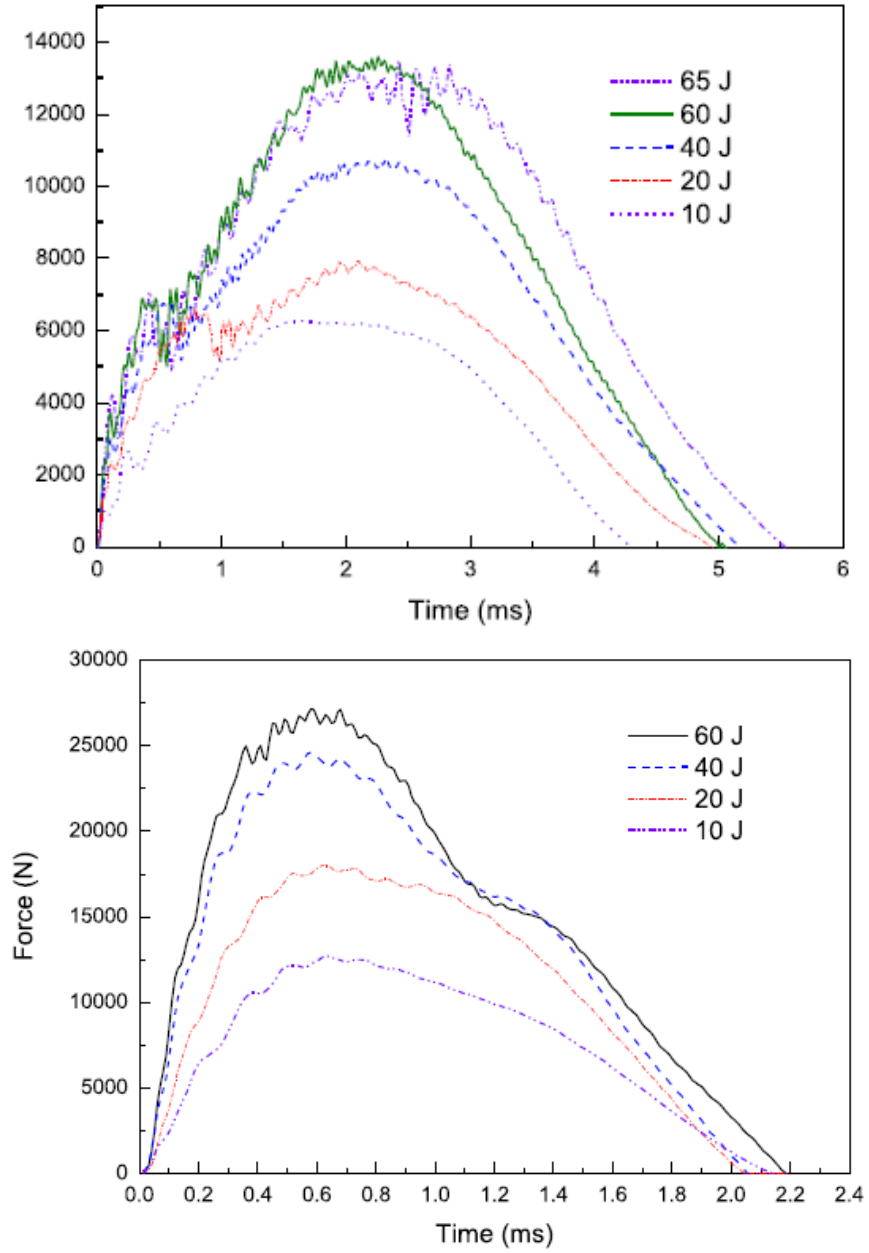

Fig. 14. Contact force histories of the type-C impact on the wing box.

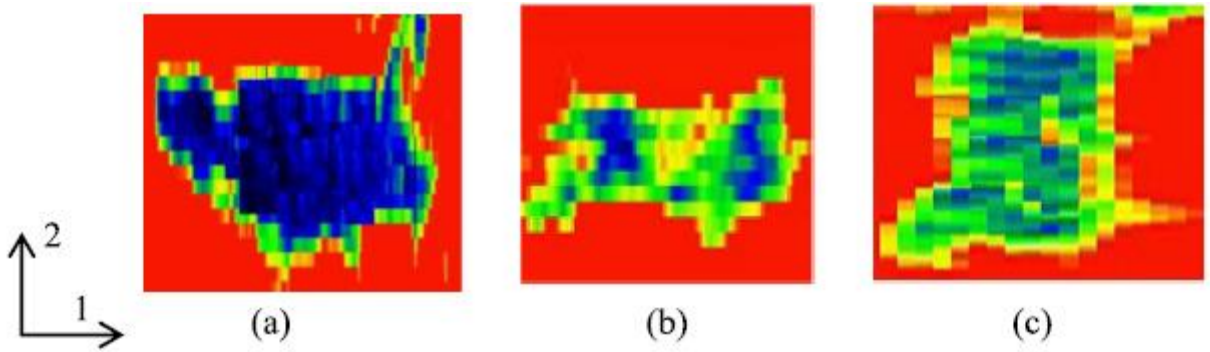

Fig. 5. Ultrasonic C-scans of the delaminations under the 40-J impacts: (a) type A, (b) type B, and (c) type C.

Table 2
Dimensions of the damage area of the wing box.

Impact type	Impact energy (J)	Dimensions of damage area along direction 1 and direction 2 (mm × mm)
A	15	27.8 × 16.5
	20	21.0 × 23.3
	40	38.3 × 27.1
	60	33.8 × 26.3
B	20	45.8 × 23.3
	40	30.8 × 12.8
	65	40.5 × 18.8
C	20	9.0 × 7.5
	40	13.5 × 11.3
	60	15.0 × 19.5

Table 3
DTL prediction for type B for the wing box.

Impact energy (J)	Experimental DTL for type A (N)	Experimental DTL for type B (N)	Predicted DTL for type B (N)	Prediction error/%
65	–	7059	–	–
60	6395	7049	7449	5.7
40	5946	6773	6926	2.3
20	5579	6608	6498	1.7
15	5290	–	6162	–
Average	5802	6872	6758	1.7

3.4. Prediction of DTL for Type-B Impact

- To predict the DTL of type-B location with the experimentally determined DTL of type-A location

3.5. The Impact Indentation

- General visible indentation occurs :
  - at 55 J for the Type-A impact
  - at 65 J for the Type-B impact.
    - Indentation is barely visible under 60 J
    - But cracks are generated on the surface
  - No indentation for the type-C impact
    - But a scar due to the high contact force

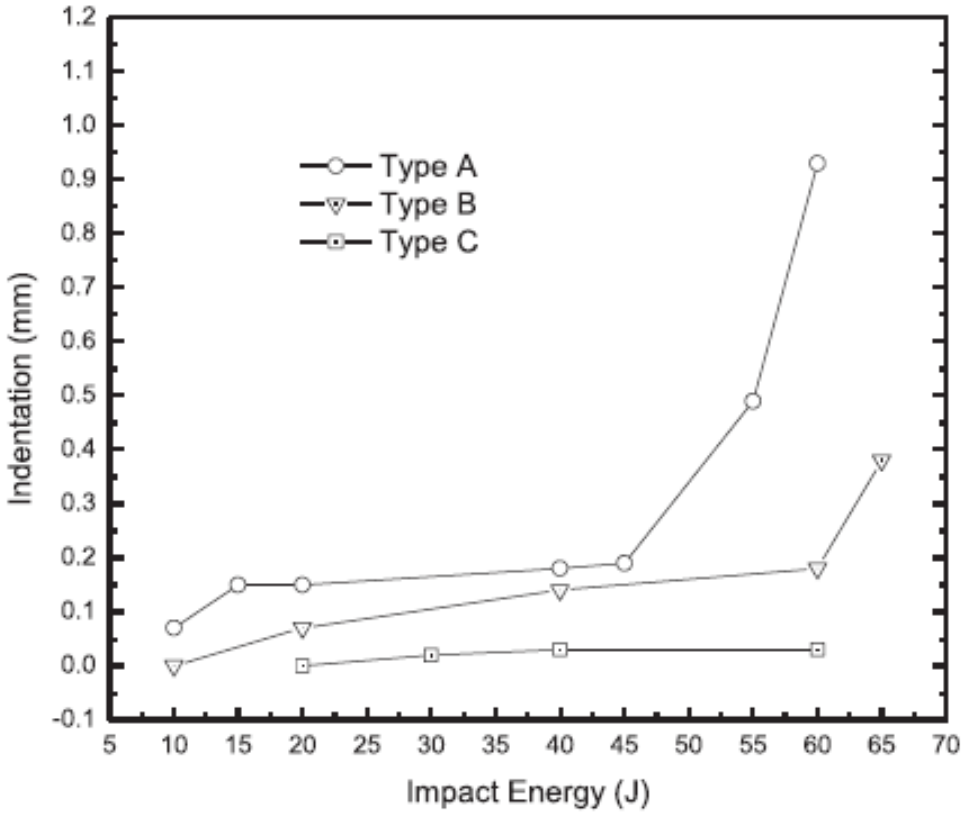

Fig. 19. Comparison of indentations of impacts on the wing box.

4 Ultimate Load Test After the Low-Velocity Impact

- A limited bending moment of 0.5x105 Nm is applied to second wing box without damage first.
- Five impact tests of 60 J is conducted on the upper surface of the wing box.
- Bending is applied to the wing box with impact damage
  - Breaks along the line at the bending moment of 1.1x105 Nm.
- Impact damage does not weaken the wing box to bear the limited load.
- The critical load of buckling of wing box is ~ 0.8x105 Nm.

Table 5
Size of delamination area.

Impact point	Impact type	Size of delamination area (mm)
P1	Type C	Φ20
P2	Type A	Φ50
P3	Type B	60 × 45
P4	Type C	Φ40
P5	Type B	75 × 40

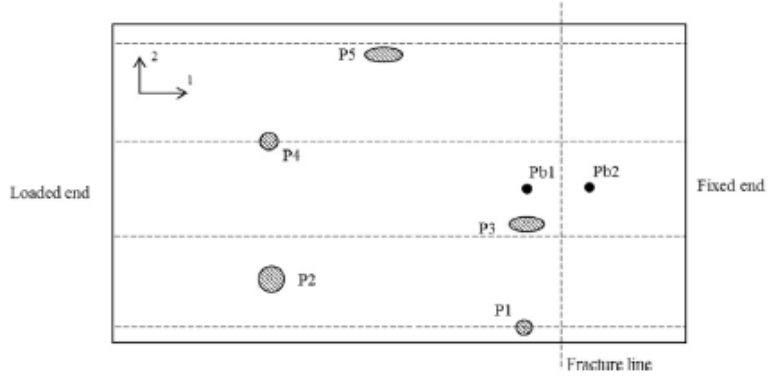

Fig. 20. Impact points and delamination regions of the wing box.

5 Conclusion

This study investigated:

- the contact force, energy absorption, delamination, and indentation due to low-velocity impact on the panel of a composite wing box.

- The characteristics of Type-A impact are consistent with the standard test on the specimen.

- The sharp drop in the F–t curve for Type-A & Type-B impacts → Causes delamination

- Very high contact force is generated by the Type-C impact
  - Size of the delamination area is small
  - Shallow indentation is observed.

- The energy absorption is high for the impacts on the horizontal tail.
- The proposed model is effective in predicting the DTL of the Type-B impact with the experimentally determined DTL of Type-A
- To investigate the behavior of the damaged region under compressive load, impact damage is applied to the wing box.

- The wing box was broken after it began to buckle.
  - The strain response at the other impact points exhibited good damage resistance to Type-B and Type-C impacts.

- The failure position is close to the supporting end
  - Rather than the impact point where the delamination propagation occurs.
  - The impact point should be located in this region when investigating the effects of the impact damage on ultimate load of composite panel.

Co-Curing Process Combining Resin Film Infusion with Prepreg and Co-cured Interlaminar Properties of Carbon Fiber Composites

1 Introduction

- The carbon fiber/epoxy resin matrix composite laminates are fabricated using a co-curing process combining resin film infusion (RFI) process with prepreg-autoclave process (co-resin film infusion)
  - Low-cost for advanced composite structure
  - High mechanical performance

- Co-cured liquid composite molding (co-LCM) is an integral forming technique for combining liquid molding process with prepreg curing process.
  - The co-LCM technology improves the processability of complex structure
  - Reduces fasteners, assembling procedures and simplifying mold → Achieves time and cost saving

- This papers:
  - Develops co-LCM in co-RTM → To fabricate aircraft structures
  - Proposes a new idea of co-RFI
    - Co-cures RFI part with prepreg stack take advantages of cost-effectiveness of RFI and high properties of unidirectional prepreg.
- Two kinds of resins are used during co-LCM process:
  - Resin in prepreg stack
  - Resin for infusion
- Co-cured laminate was compared with RFI laminate and prepreg laminate:
  - Processing quality
  - Mode I and Mode II interlaminar fracture toughness

2 Experiment

2.1 Materials:

- A kind of epoxy resin film (MTM 44-1)
- T700SC (12k tow) unidirectional carbon fiber (for RFI process)
- HTS 5631 (12k tow)/MTM 44-1 unidirectional prepreg (for this study)
- An epoxy tackifier (for binding CFW-200 fabrics in RFI process and powder form)

2.2 Composite Manufacturing:

Prepreg-autoclave process:

- MTM 44-1 is cured with teflon film (To form pre-crack)
- Rrecommended cure cycle was applied in autoclave. Vacuum is applied.
- Temperature is increased:
  - Room temperature to 180°C at 2°C/min and maintained at 180°C for 2 h.

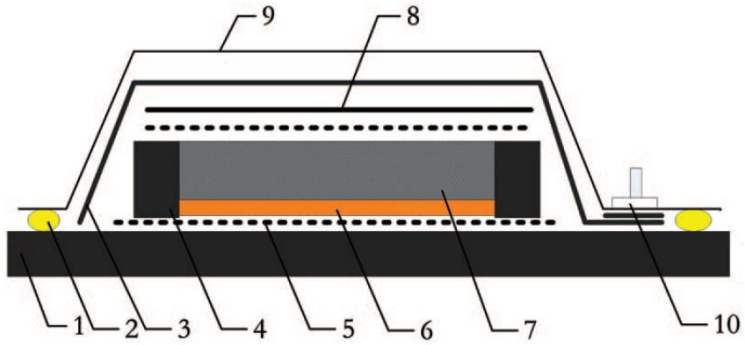

Figure 1. Schematic of the bagging procedure in RFI process.
1 – steel plate, 2 – sealant, 3 – breather, 4 – dam, 5 – peel ply, 6 – resin film, 7 – fiber fabric, 8 – release film, 9 – vacuum bag, 10 – vacuum valve.

RFI process:

- The stack contains 20 layers of CFW-200 (in 0 direction) and nine layers of resin film
- The release film was used → To ensure entrapped air to be released.
- Teflon film was placed in mid of the fiber stack.

1. Process A: Heat from 25°C to 180°C at 2°C/min and hold at 180°C for 120 min. (Recommended by manufacturer)

2. Process B: Heat from 25°C to 130°C at 2°C/min and hold at 130°C for 30 min. Then, increase to 180°C at 2°C/min for 120 min.

3. Process C: Disperse 8wt% tackifier on the surface of CFW-200 and maintain 5 min at 80°C. Then, the same cure cycle as Process B.

Co-RFI process:

- 16 MTM 44-1 prepreg layers, 10 CFW-200 fabric plies and five layers of resin film (in 0 direction)
- Two kinds of lay-up types: Prepreg layers at the top of stack (prepreg/RFI) , Prepreg layers on bottom of stack (RFI/prepreg)
- Manufactured in an autoclave using Process A, B and C.

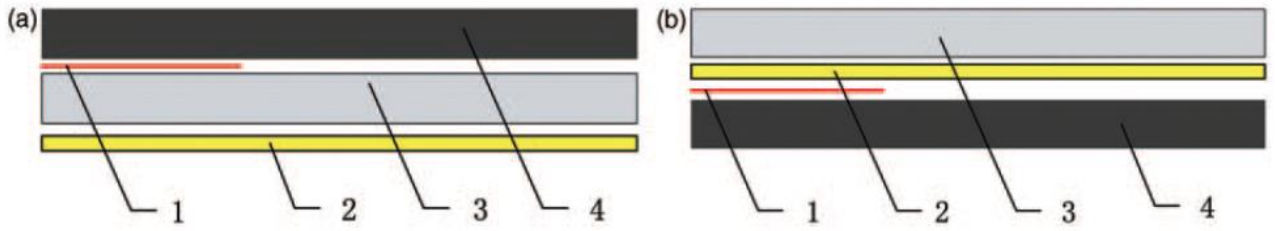

Figure 3. Schematic of two kinds of lay-up types: (a) prepreg/RFI stack and (b) RFI/prepreg stack. 1 – Teflon film, 2 – five layers of resin film, 3 – 10 carbon fiber fabric plies, 4 – 16 prepreg layers.

3 Testing

3.1 Resin Viscosity

- Using a Gemini rheometer

3.2 Mode I Interlaminar Fracture Toughness

- Using the double cantilever beam (DCB) specimen
- DCB specimen Width = 25mm and Length = 150mm
- The critical G_{IC} is calculated as average of G_{IC} values at beginning of delamination

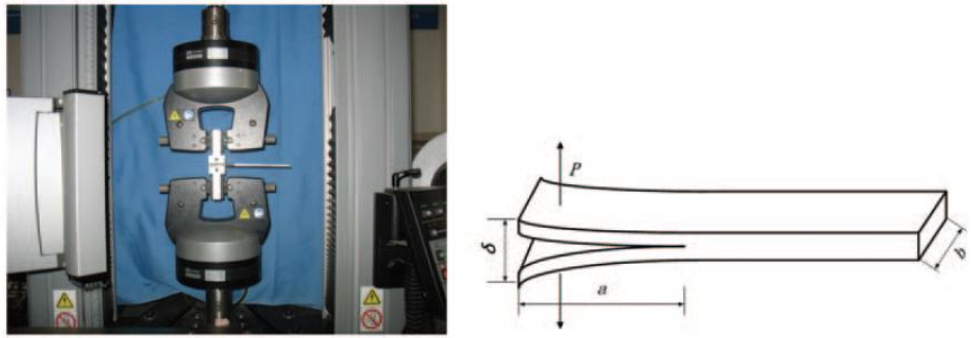

Figure 4. Schematic of DCB testing: a = crack length, p = Load, δ = displacement.
DCB: double cantilever beam.

3.3 Mode II Interlaminar Fracture Toughness

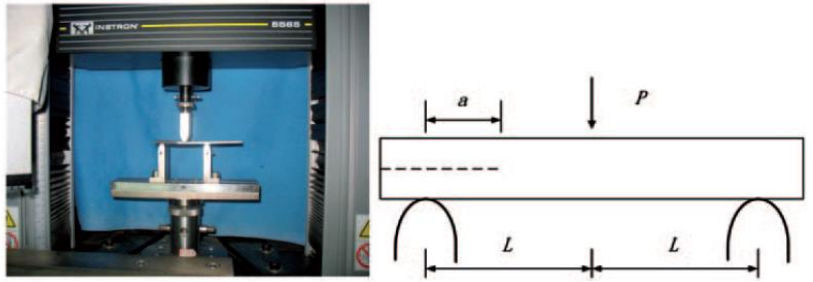

Figure 6. Schematic of ENF testing: a = the effective crack length, p = load, L = a half of the span length. ENF: end notched flexure.

- Using the end notched flexure (ENF) specimen.
- The ENF specimen; Width = 25mm and Length = 140mm
- Initial G_{IC} is calculated as average of G_{IC} values using the crack initiation loading for each specimen group

3.4 Processing Quality Observation

- Observation by
  - Optical micrograph → To observe defects inside laminates
  - Laminate thickness
- Using scanning electron microscopy → To observe crack surface of samples

4 Results and Discussion

Table 3. The void content of different laminates.

	Void content (%)		
	Process A	Process B	Process C
RFI laminate	0.03	0.02	0.01
RFI/prepreg laminate	0.03	0.01	0.01
Prepreg/RFI laminate	0.86 ± 0.03	0.63 ± 0.02	0.59 ± 0.01
Prepreg laminate	0	–	–

4.1 Processing Quality of Co-Curing Process

- Quality of prepreg laminate is perfect without void and the prepreg/RFI laminate cured by Process A gives the maximum value (about 0.86%)
- Void contents in co-cured interface are higher than integral laminates (especially for prepreg/RFI laminates)
- Isothermal dwell (in Process B) has great influence on decrease of voids at the laminate
- Addition of the tackifier almost has no influence on the flow and infiltration of the matrix resin
  - But makes the resin more redundant than the laminates without tackifier.

4.2 Evaluation Of Co-RFI Laminate Interface

- G_{IC} of RFI/prepreg laminate is 192 J/m2.
- G_{IC} of prepreg/RFI is 190 J/m2.
- Prepreg laminate has the maximum critical G_{IC}(222 J/m2).
- RFI processed laminate gives the minimum G_{IC} (168 J/m2).
- The cracks in the prepreg laminate runs along the centerline without deflection.

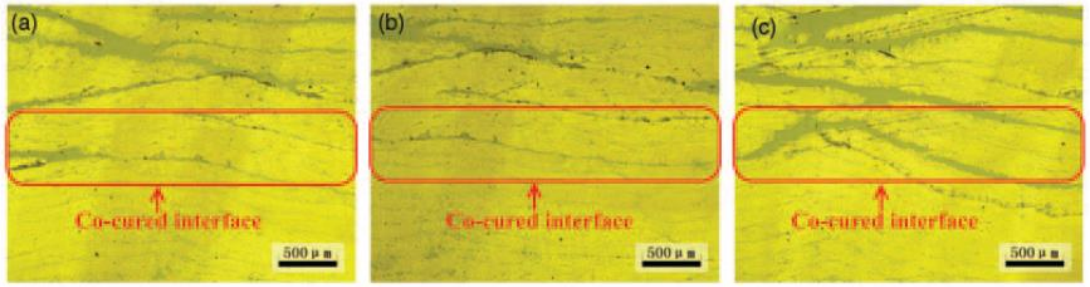

Figure 10. Micrographs of RFI/prepreg laminates cured by: (a) Process A, (b) Process B and (c) Process C. RFI: resin film infusion.

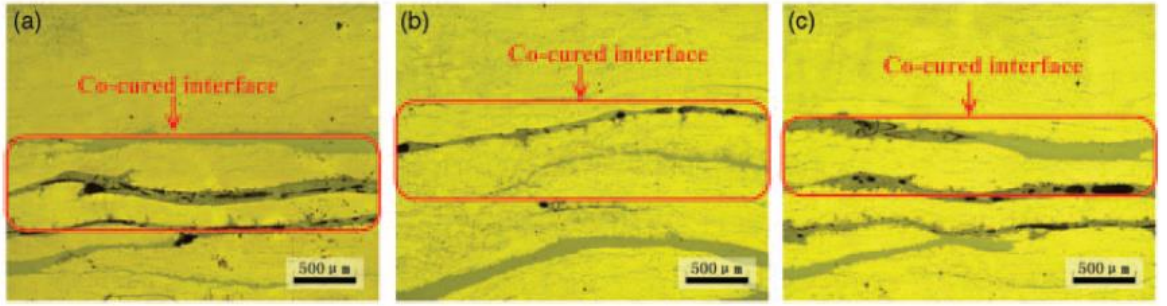

Figure 11. Micrographs of prepreg/RFI laminates cured by: (a) Process A, (b) Process B and (c) Process C.

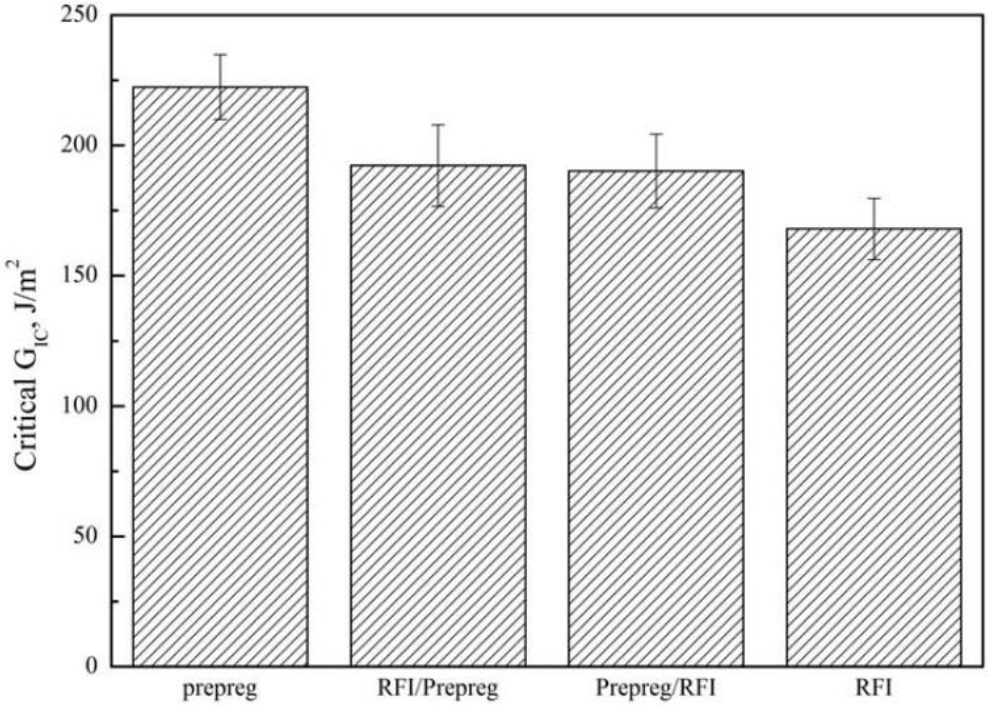

Figure 13. The critical G_{IC} values of different laminates fabricated using Process A.

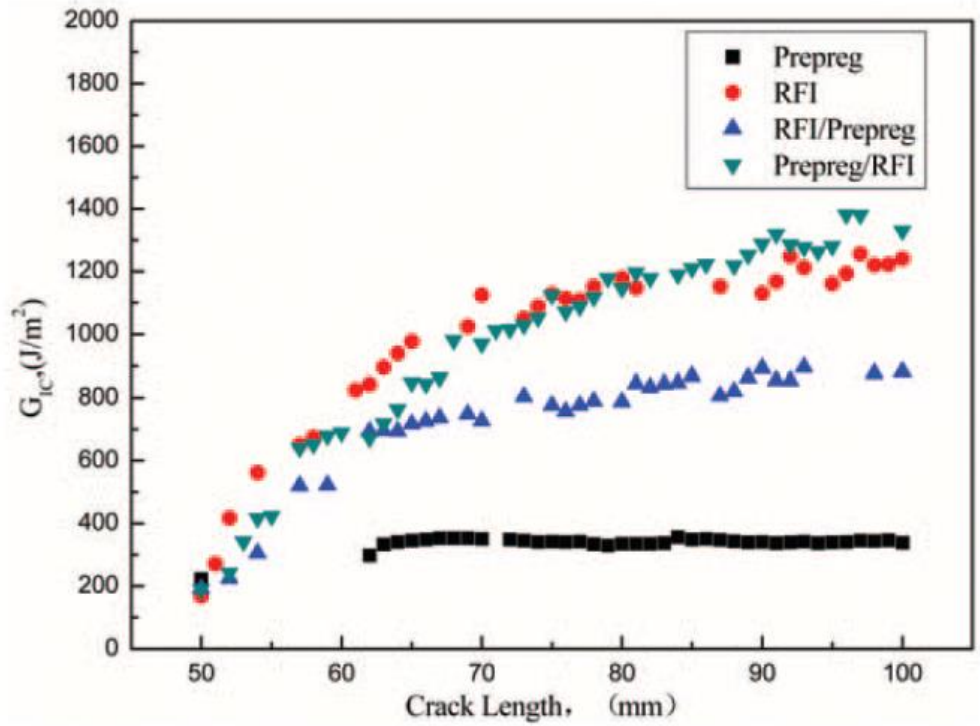

Figure 14. Mode I delamination resistance curves (R-curves) of laminates cured by Process A.

4.3 Influence Of Isothermal Dwell And Tackifier On The Interlaminar Properties

- The laminates co-cured under Processes B and C are tested through the Mode I and Mode II interlaminar fracture toughness

- The effects of the isothermal dwell and the tackifier on the interlaminar properties of co-cured interface are evaluated.

Influence Of Isothermal Dwell:

- Initial G_{IC} of co-RFI laminates fabricated using Process A and B.
- Significant increase in the initial G_{IC} for the composite laminates cured by Process B, compared to Process A.

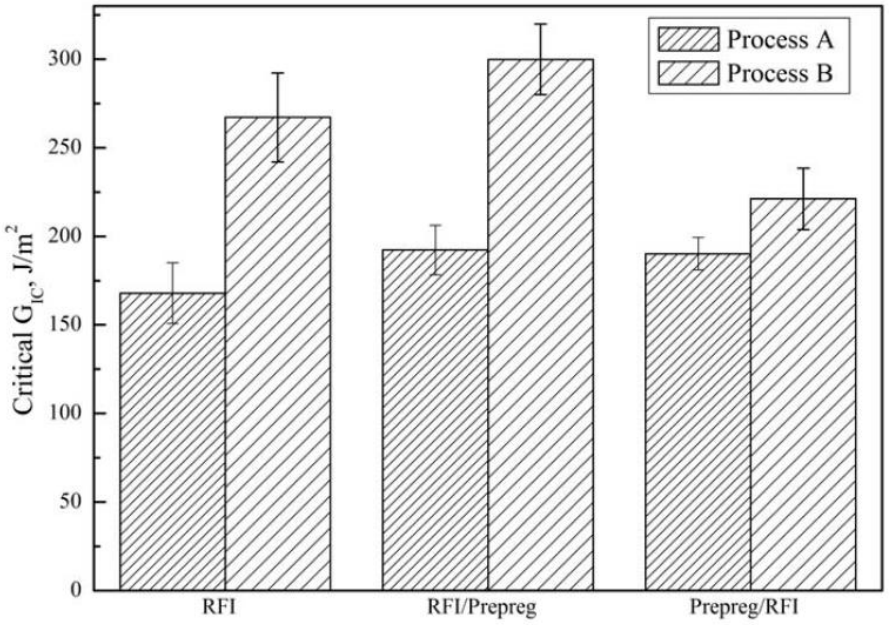

Figure 17. The initial G_{IC} values of laminates cured by Process A and Process B.

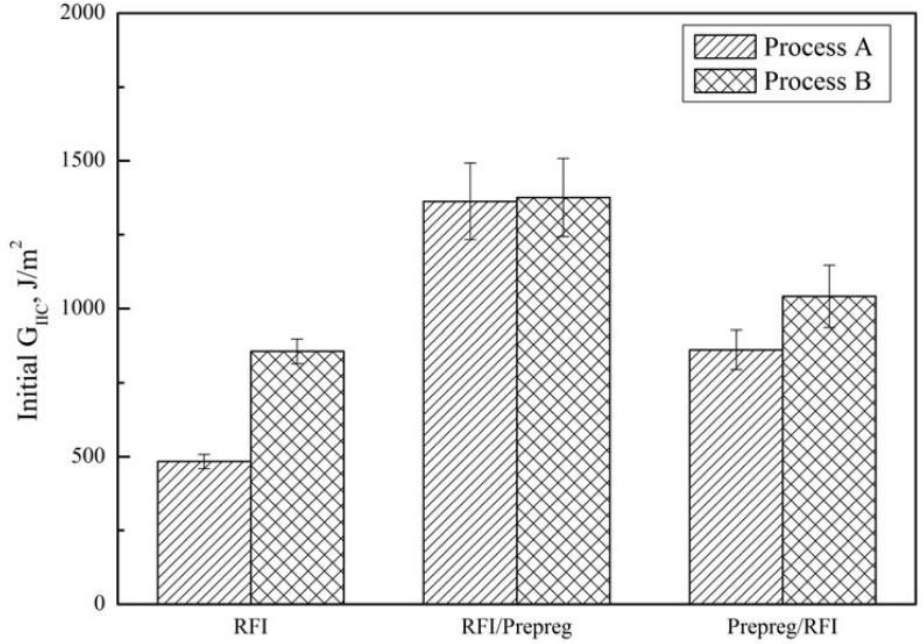

Figure 19. The initial G_{IIC} values of laminates cured by Process A and Process B.

Influence Of Tackifier:

- Tackifier has effect on the interlaminar fracture toughness of laminates.
- Initial G_{IC} of RFI laminate with tackifier is improved compared with the RFI without tackifier
- But initial G_{IC} values of co-RFI laminates with tackifier decrease in contrast with co-RFI without tackifier.

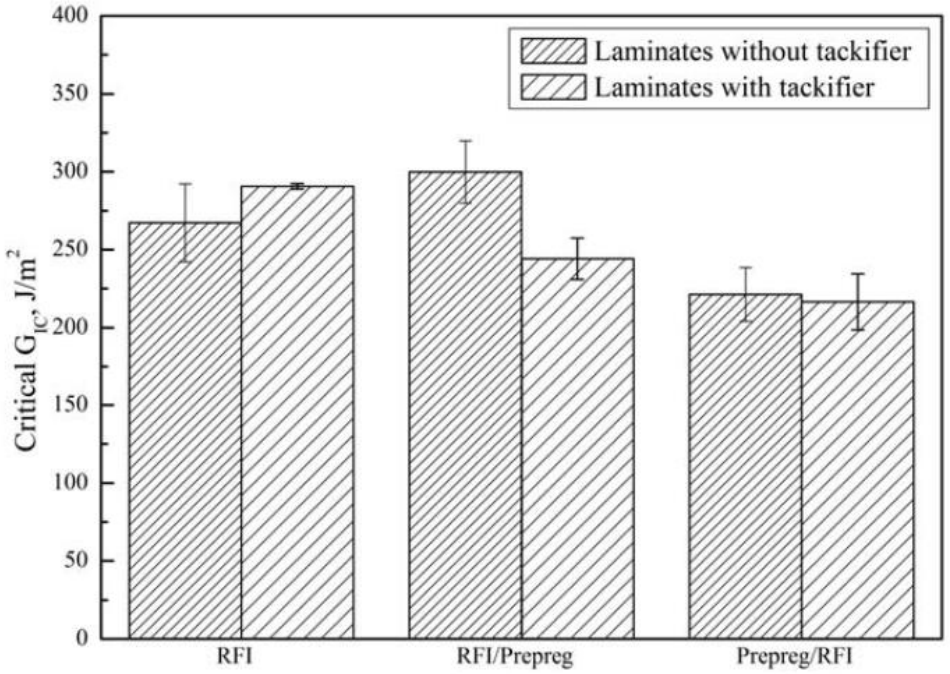

Figure 20. The critical G_{IC} values of laminates cured by Process B and Process C.

Table 5. The initial G_{IC} values of laminates cured by Processes A, B and C.

	The initial G_{IC} values		
	Process A	Process B	Process C
RFI laminate	167.96 ± 17.09	267.17 ± 25.09	290.59 ± 1.84
RFI/prepreg laminate	192.28 ± 14.01	299.87 ± 19.95	244.15 ± 13.21
Prepreg/RFI laminate	190.18 ± 9.10	221.17 ± 17.35	216.44 ± 17.93

RFI: resin film infusion.

Table 6. The initial G_{IIC} values of laminates cured by Process A, B and C.

	The initial G_{IIC} values		
	Process A	Process B	Process C
RFI laminate	547.96 ± 21.58	1159.90 ± 53.34	1838.77 ± 72.05
RFI/prepreg laminate	1414.77 ± 78.15	2031.17 ± 135.70	2553.02 ± 109.44
Prepreg/RFI laminate	1155.205 ± 46.37	1776.62 ± 169.335	984.44 ± 126.98

RFI: resin film infusion.

5 Conclusion

- Optical photographs of the laminates cured by co-RFI shows
  - Matrix-rich regions and voids mostly exist in RFI part and the interlaminar interface between the prepreg part and RFI part.
  - The matrix-rich regions and voids at the co-cured interface reduce the interlaminar properties of the co-RFI laminates, causing a lower delamination resistance

- Isothermal dwell before curing process has a great influence on the interlaminar fracture toughness of co-RFI laminates
  - Improves the interlaminar fracture toughness → Due to low resin viscosity and infusion time for improving the impregnation degree of the fiber preform.

- Epoxy tackifier is an important factor to make the resin redundant
  - Enlarges the matrix-rich region at the co-cured interface, and changes the interlaminar fracture toughness.

An Analytical Model For B-Stage Joining and Co-curing of Carbon Fibre Epoxy Composites

1 Introduction

- Paper develops cure kinetic models
  - To describe the B-stage curing
  - Co-curing assembly of **carbon fibre reinforced thermosetting polymer** (CFRP) composites
- **Problem** of using CFRP materials:
  - Inefficient joining procedures
  - Strict certification standards

  } Lost in efficiency

- **The solution**:
  - To partially cure two subassemblies, combine them and complete the cure cycle for both

- Co-cured joints have higher fracture toughness and joint strength than co-bonded joints
- Cure kinetic modelling of thermoset resins is widely used
- Most works focus on wide temperature ranges, model optimization for a wide range of degree of cure
  - Such models are insufficent for B-Stage curing and co-curing (due to variance in a few degrees)
- A new approach is proposed to describe B-Stage curing and co-curing assembly by using developed kinetic model

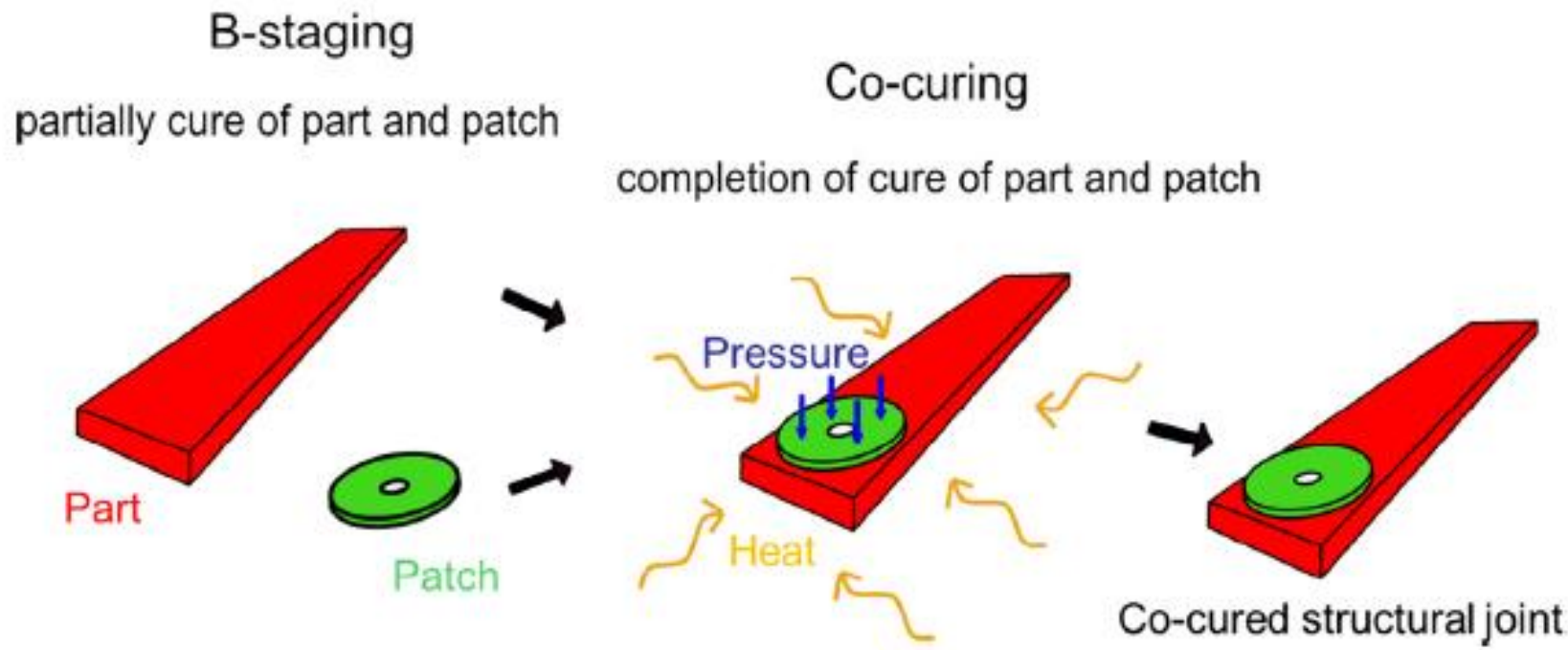

Fig. 1. Shows the concept of patch reinforcement of a structural part via co-curing of B-stage cured components. (For interpretation of the references to colour in this figure legend, the reader is referred to the web version of this article.)

2 Materials

- **Resin:** HexFlow RTM6
- **CFRP parts:** Manufactured by a RTM process
- **Reinforcing CFRP patches:** Manufactured from thin ply material
- **Nylon peel:** To prepare surfaces for co-curing

3 Experimental

- The differential scanning calorimetry (DSC) measurements were made

3.1 Resin Cure Kinetics

- Isothermal and dynamic DSC measurements of the uncured resin were made as reference data for the analytical modelling

3.2 B-stage Degree Of Cure

- The resin was heated to 80° C for one hour
- Transferred to a plate heated vacuum oven
- Degassed to 20 kPa for five minutes
- Circa 0.8 kPa vacuum pressure for a further 25 min

- The CFRP parts were cured at 400 kPa for varying times at 160°C
- Completely cured parts were cured at 180°C for 90 minutes in the RTM tool
- The B-stage cured CFRP parts were cured at 160°C in the RTM tool

3.4 Co-Curing Of the CFRP Part and Patch

- The CFRP patch and CFRP part were prepared by first removing peel plies (for adhesive)
- Two components were assembled in a silicone ring sealed compression jig.
  - Encasing the CFRP patch to a net shape with hole
  - Applying consolidation pressure (2 MPa) to provide intimate contact of the CFRP part to the patch

4. Models and Methodology

- The curing reaction is applied using DSC of the pure resin at different temperatures and heating rates .
- Kinetics of the curing reaction of the resin are investigated.

4.1. Model For Evolution Of T_g and Resin Cure Kinetics

- DiBenedetto model is used to describe T_g as a function of α (degree of cure).

4.2. B-Stage Curing Cycle Of the CFRP Part and Patch

- The part and the patch being joined, both were cured at 160 C.

4.3. Co-Curing Cycle Of the CFRP Part and Patch

- Heating rate is reduced to 1°C/min
- After 180 C, temeperature is held for 60 minutes
  - To ensure full crosslinking in both the part and the patch.

5 Result

5.1 DSC Measurements

- The maximum heat of reaction at a cure temperature, ΔH_{iso}, was first determined using isothermal measurements.

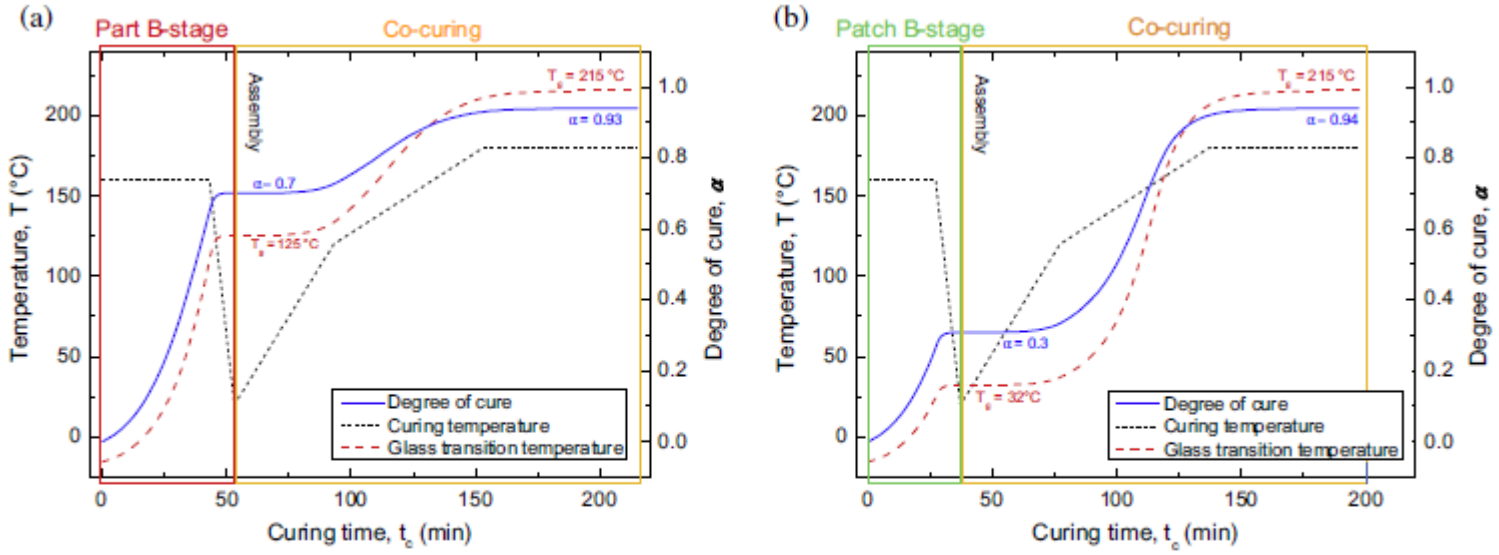

Fig. 6. Curing cycle for the (a) part and (b) patch, showing that the glass transition temperature, T_g, of the part is always above the curing temperature, T_c whereas the T_g of the patch is far below and allows the resin to flow. (For interpretation of the references to colour in this figure legend, the reader is referred to the web version of this article.)

- **5.2 Comparison Of The Measured And Predicted B-Stage**

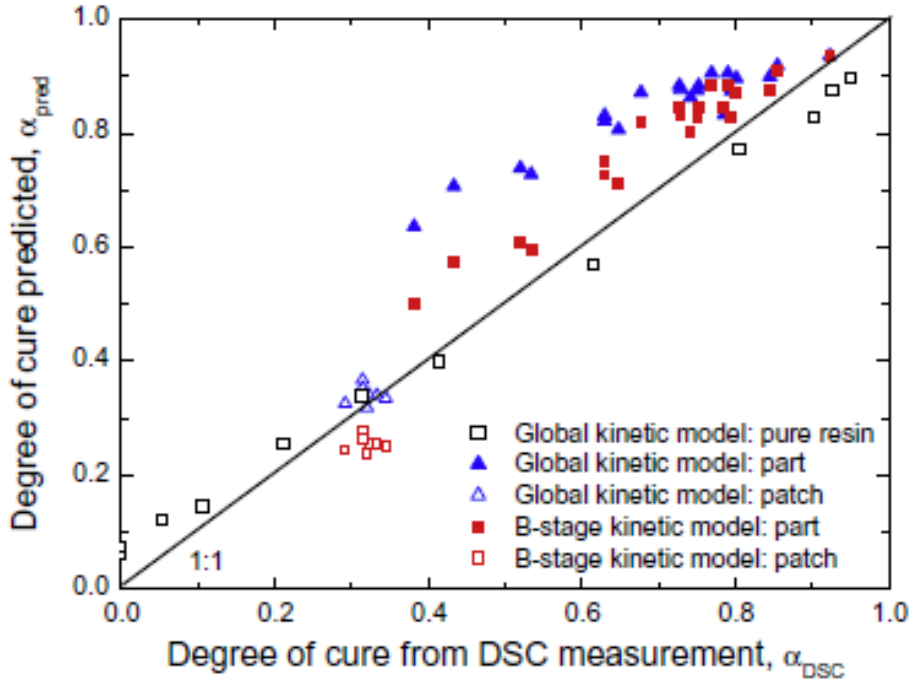

Fig. 7. Modelled values of degree of cure, α, versus those measured using DSC using both the global kinetic model based on isothermal measurements from 120 to 180 °C, and the improved B-stage kinetic model based on isothermal measurements in the range 154–166 °C (based on mould temperature sensor close to cavity in composite processing). (For interpretation of the references to colour in this figure legend, the reader is referred to the web version of this article.)

- The kinetic model was optimized for the temperature range of 154–166°C.

5.3 Co-curing Of The CFRP Part And Patch

- The interface between the CFRP part and CFRP patch is indicated by the red dotted line.
- Void free bond was possible → No evidence of porosity in the interface between part & patch
- Damage accumulation in right side displays the evidence of kink bands due to compression stresses.

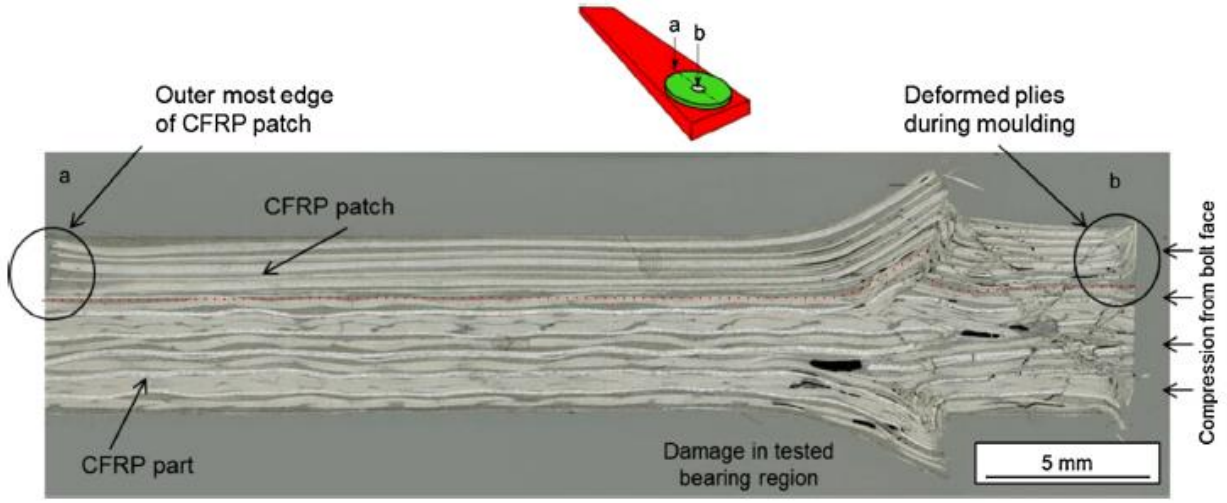

Fig. 8. Optical micrograph of the assembled, co-cured CFRP part to the CFRP patch after a double lap bearing test. Red indicates the interface between the two components. (For interpretation of the references to colour in this figure legend, the reader is referred to the web version of this article.)

5.4 Discussion

- B-stage cure profiles were successfully applied to the the epoxy resin
- The progression of α and T_g were successfully described when compared to measurements using DSC.
- Accurate temperature monitoring is required → To reach required precision.
- Best results were obtained with 30% cured B-stage patches and 75% cured B-stage parts

6 Conculusion

- This work demonstrated an approach for using the developed kinetic model to describe the B-stage curing and co-curing assembly of local reinforcement.

- Described methodology to locally reinforce a partially cured structure has proved to be possible and presents techniques that are readily scalable, and cost effective.

- **Biggest challenge** for industrialisation is to the narrow window for the free standing cure of the CFRP part presented by the RTM6 resin system.